Monolayer dispersion of oxides and salts on surface of ZrO_2 and its application in preparation of ZrO_2-supported catalysts with high surface areas

Bi-ying Zhao *, Xian-ping Xu, Hua-rong Ma, Don-hong Sun and Jin-ming Gao

Institute of Physical Chemistry, Peking University, Beijing 100871, PR China
E-mail: zhaoby@csb0.ipc.pku.edu.cn

Received 24 October 1996; accepted 19 March 1997

The thermostability of ZrO_2 can be improved by dispersing a layer of an active component onto its surface in advance. The research results of seven kinds of catalysts (ZrO_2-supported MoO_3, WO_3, CuO, SO_4^{2-}, NiO, $FeSO_4$ and Fe_2O_3) show that the surface areas of the samples prepared by impregnating $Zr(OH)_4$ with the active components and then calcining at high temperature are much larger than those of the samples prepared with an ordinary method, namely, impregnating ZrO_2 calcined at high temperature. The surface areas of the ZrO_2-supported catalysts obtained in this way are several times that of pure ZrO_2 calcined at the same temperature. The characteristic results show: (1) the active components are dispersed on the surface of ZrO_2 as monolayer; (2) there is a good corresponding relationship between the surface coverage and the surface area of the sample; (3) as the loading of an active component comes up to its utmost dispersion capacity, the surface area of the sample will be the largest. The mechanism responsible for these phenomena has been discussed.

Keywords: monolayer dispersion, ZrO_2-supported catalysts, highly specific surface

1. Introduction

An ordinary method of preparing oxide-supported catalysts is that the support is calcined in order to turn the hydrous oxide into the oxide and stabilize its texture, then it is impregnated with the solution of an active component and calcined again. The pre-calcination temperature of the support is often equal to or higher than the one at which the resulting catalyst is treated. For some classical supports such as γ-Al_2O_3 and silica gel, using this method one can easily obtain supported catalysts with high surface areas (150–300 m^2/g). Recently, zirconia as support is attracting considerable interest [1]. However, it is very difficult to obtain ZrO_2-supported catalysts with high surface areas, because its original surface area is not very large and decreases rapidly during calcination at high temperature. Thus, its applications are thereby limited.

Recently, it has been realized that crystallite growth, accompanying phase transformation and inter-crystallite sintering should be responsible for degeneration of the texture of a support during calcination, and these processes occur via a mechanism of surface diffusion [1]. Several years ago, our research group proved that many oxides and salts can disperse onto surfaces of supports as a monolayer [2–4]. So we image that if a layer of active component is dispersed on the surface of a support to segregate the particles of the support from each other before the particles have grown into bigger ones, its surface diffusion would be suppressed, and the thermostability of its texture would be improved, and as a result, a catalyst with high surface area would be obtained.

We reported that a MoO_3/TiO_2 catalyst with high surface area was obtained by adding a solution of $(NH_4)_6Mo_7O_{24}$ to $Ti(OH)_4$ and then calcining it at 500°C for 4 h [5]. For example, the surface area of the catalyst with 13 wt% MoO_3 is 133 m^2/g. However, the surface area of MoO_3/TiO_2 (with same MoO_3 content) obtained by impregnating TiO_2 crystallized at 500°C and then calcining at the same temperature is only 66 m^2/g. We were also attentive to other authors' works and found some data that can be used to support our ideal. For example, Arata and Hino [6,7] prepared many new solid superacids by impregnating $Zr(OH)_4$ with aqueous $(NH_4)_6(H_2W_{12}O_{40})$, $(NH_4)_2SO_4$ or $(NH_4)_6Mo_7O_{24}$, followed by evaporating the water, drying and then calcining at high temperature. From the papers they published we noticed that the surface areas of these superacids were much larger than that of pure ZrO_2 treated at the same temperature. In addition, Cimino et al. reported that CrO_3 addition can display a protective effect on the surface areas of specimens based on ZrO_2 only dried at 110°C [8].

In recent years, the method of doping of some oxides (surface doping or bulk doping) was used in studies on superplastic ZrO_2 ceramics [9] and SnO_2 gas-sensitive materials [10–12] to improve their thermostability and

* To whom correspondence should be addressed.

microstructure, and some inspiring results were obtained.

These facts indicate that the surface areas of the samples obtained by impregnating hydrous zirconia and then calcining are often larger than those of the samples obtained by impregnating the crystalline oxide. However, to date there have not been published systematic and detailed reports about it in the catalytic literature. Therefore, it is important to prove the generality of this phenomenon, to explore its origin and rule, and to make use of it to prepare some catalysts with high surface areas. In this paper, we will report the research results on several ZrO_2-supported catalyst systems that are valuable in application.

2. Experimental

2.1. Sample preparation

A solution of ammonia (3.3 M) was added dropwise into a solution of zirconyl chloride (1 M) under stirring until pH = 10. The precipitate was aged in the mother liquor for 24 h, then filtered and washed repeatedly with distilled water until a negative test for chloride ions was obtained. The chloride-free hydrogel was dried in air at 110°C for 24 h, then ground to proper particle size.

MoO_3/ZrO_2, WO_3/ZrO_2, CuO/ZrO_2, SO_4^{2-}/ZrO_2, Fe_2O_3/ZrO_2, NiO/ZrO_2 and $FeSO_4/ZrO_2$ were prepared by impregnating the dried hydrogel with solutions of ammonium heptamolybdate, ammonium metatungstate, copper nitrate, ammonium sulfate, iron nitrate, nickel nitrate and iron sulfate respectively, then drying and calcining at designated temperature for 4 h.

For comparison, a portion of $Zr(OH)_4$ was calcined at 450–800°C for 4 h to turn it into ZrO_2, and some catalysts were prepared by impregnating the obtained ZrO_2. $Zr(OH)_4$ samples used in different catalyst systems were made in separate batches, therefore their specific surfaces are slightly different.

2.2. Sample characterization

X-ray diffraction. The identification of phases was carried out by means of a BD-86 X-ray diffractometer, employing Cu Kα (Ni-filtered) radiation.

Surface area measurement. The surface areas (SA) of all samples were measured using the BET method by N_2 adsorption at 77 K. Resultant surface areas were normalized to the values per gram support in order to compare with each other.

Raman spectra determination. Raman spectra were obtained with a Jobin-Yvon U-1000 monochromator. The 514.5 nm line of a Spectra-Physics model Stabilite-2016 Ar^+ laser was used for excitation. A laser power of 100 mW and the spectral slit width of 1 cm^{-1} were applied.

XPS measurement. XPS spectra were obtained with a VG-ESCALAB5 spectrometer. As anode, Al Kα was employed, usually at 10 kV, 40 mA. The specimen was treated at 10^{-8} Torr. The energy of analysis chamber was fixed at 50 eV. The XPS peak intensity ratio between an appointed energy level of some element in an active component and Zr 3d was taken as a measurement of the surface concentration of the active component on ZrO_2.

DTA determination. DTA measurements were performed by a Dupont model 1090 apparatus, using α-Al_2O_3 as reference and a temperature rise rate of 20 K/min.

3. Results

3.1. MoO_3/ZrO_2 systems

3.1.1. BET surface areas

The SA of pure ZrO_2 obtained by calcining $Zr(OH)_4$ at 550°C for 4 h is 52 m^2/g. After supporting MoO_3, its SA would decrease gradually with a rise in MoO_3 content.

The relationships between SA of the samples obtained by impregnating $Zr(OH)_4$ (dried at 110°C) with $(NH_4)_6Mo_7O_{24}$ solution and then calcining at 450, 550, 600, and 750°C respectively and their MoO_3 loadings are shown in table 1. The following facts are worthy of special mention:

(a) The surface areas of these samples are several times larger than that of the pure ZrO_2 calcined at the same temperature. This phenomenon is shown clearly for the samples calcined at higher temperature. For example, the SA of MoO_3/ZrO_2 with 0.16 g MoO_3/g ZrO_2 prepared by impregnating $Zr(OH)_4$ and then calcining it at 750°C is 101 m^2/g ZrO_2, which is ten times that of ZrO_2 obtained by calcining pure $Zr(OH)_4$ at the same temperature.

(b) With the MoO_3 contents increasing, the surface areas of these samples calcined at a certain temperature increase and reach a maximum value (S_{max}), then decrease. The MoO_3 content corresponding to S_{max} depends on the calcination temperature of the sample.

Table 1
The surface areas of MoO_3/ZrO_2

MoO_3 content (g/g ZrO_2)	SA (m^2/g ZrO_2)			
	450°C	550°C	600°C	750°C
0	96	52	32	10
0.03	131	87	60	52
0.09	156	140	84	96
0.16	218	186	135	101
0.26	307	224	189	97
0.31	310	210	175	–
0.42	304	159	143	78
0.51	255	104	120	47

At a lower calcination temperature, S_{max} is larger and the correspondent MoO_3 content is higher.

(c) For MoO_3/ZrO_2, the decline of SA with a rise in calcination temperature is much slower than for pure ZrO_2. For example, as the calcination temperature rises from 450 to 750°C, the surface area of the sample containing 0.16 g MoO_3 per gram ZrO_2 reduces by two-fold, but the SA of pure ZrO_2 reduces by ten-fold. It is obvious that the presence of MoO_3 can improve the thermostability of the texture of ZrO_2.

3.1.2. The results of XRD

The results of XRD show that there is a close relationship between the phase of ZrO_2 in a sample and its MoO_3 content. From figure 1, it can be seen that the ZrO_2 obtained by calcining pure $Zr(OH)_4$ at 450°C for 4 h is a mixture of monoclinic (m) and tetragonal (t) phases; however, the fraction of ZrO_2 (t) in MoO_3/ZrO_2 with only a low content of MoO_3 increases obviously. As the content of MoO_3 is high enough, all ZrO_2 in MoO_3/ZrO_2 is tetragonal, and its XRD peaks become broader, which indicates that the ZrO_2 crystallite size gets smaller. As more MoO_3 is loaded, ZrO_2 is present as an amorphous phase.

After being calcined at 550°C, nearly all of $Zr(OH)_4$ changes into monoclinic ZrO_2. However, ZrO_2 obtained from $Zr(OH)_4$ with sufficient Mo(VI) still appears as tetragonal ZrO_2, even if calcined at 750°C (see figure 2). Obviously, Mo(VI) supported on $Zr(OH)_4$ opposes the crystallization of ZrO_2 and the tetragonal to monoclinic transition.

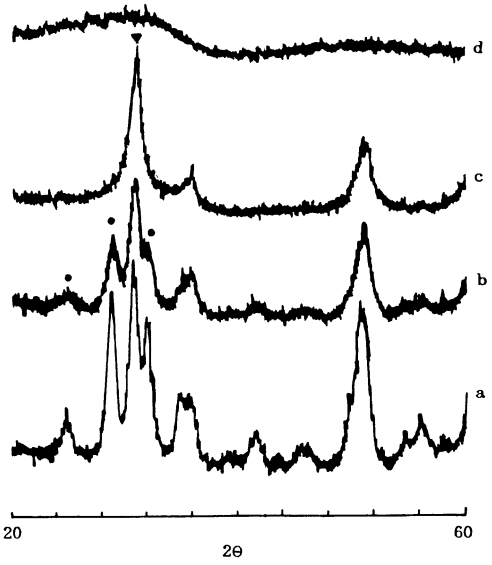

Figure 1. XRD patterns of MoO_3/ZrO_2 calcined at 450°C. MoO_3 content: (a) 0 (pure ZrO_2); (b) 0.03 g MoO_3/g ZrO_2; 0.16 g MoO_3/g ZrO_2; (d) 0.42 g MoO_3/g ZrO_2. (▼) Tetragonal ZrO_2; (●) monoclinic ZrO_2.

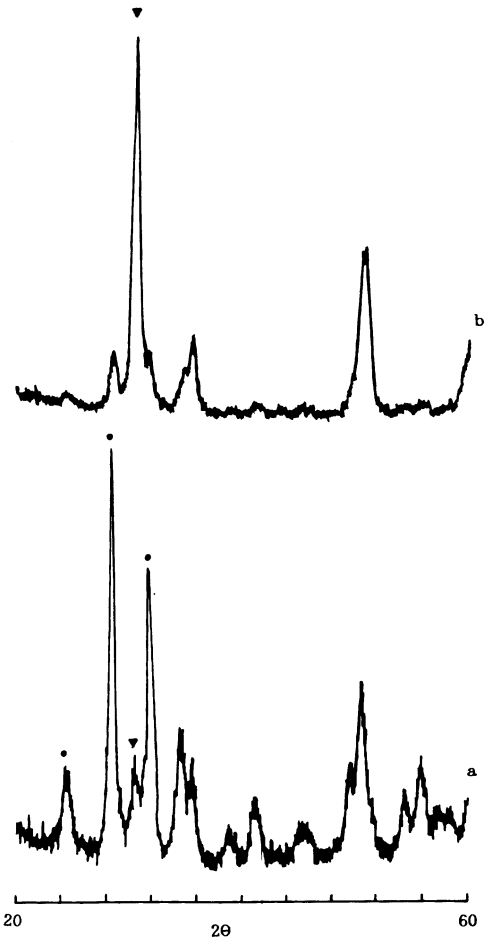

Figure 2. XRD patterns of some samples. (a) ZrO_2 calcined at 550°C; (b) MoO_3/ZrO_2 with 0.16 g MoO_3/g ZrO_2, calcined at 750°C.

3.1.3. DTA determination

The results in figure 3 show that the crystallization temperature for ZrO_2 from pure $Zr(OH)_4$ is 452°C. However, for $Zr(OH)_4$ with Mo(IV) (corresponding to 0.5 g MoO_3/g ZrO_2), the crystallization temperature of ZrO_2 increases by about 150°C, which means that the supported MoO_3 delays the crystallization process of ZrO_2.

3.1.4. Results of Raman spectra

Raman spectra results for the phase of the support are corresponding to the XRD results. In addition, the results show that MoO_3 in MoO_3/ZrO_2 is dispersed on ZrO_2 as a monolayer. In the Raman spectra, a broad band at ~ 950 cm^{-1} is observed, which is assigned to a two-dimensional polymeric molybdate [13,14], and an additional broad band at ~ 814 cm^{-1} attributed to a Mo–O–Zr surface species appears [15]. Only when MoO_3 loading is above a certain level and the calcination temperature is over 500°C, a group of sharp peaks of bulk $Zr_2(MoO_4)_2$ at 750, 946, 1002 cm^{-1} appear (see figure 4). In this case, bulk $Zr_2(MoO_4)_2$ is also identified by XRD.

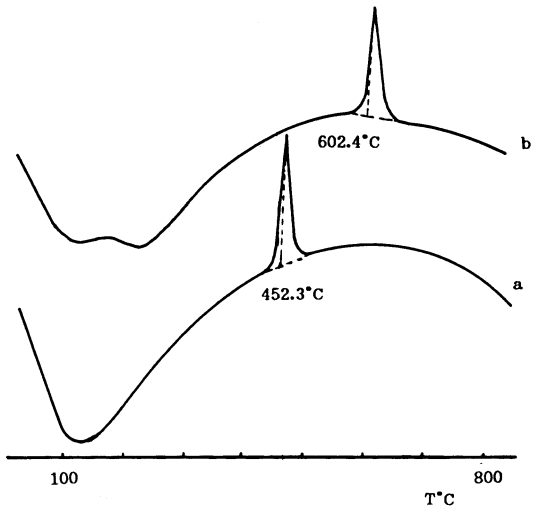

Figure 3. DTA results of $Zr(OH)_4$ and $Zr(OH)_4$ with $(NH_4)_6Mo_7O_{24}$. (a) $Zr(OH)_4$; (b) $(NH_4)_6Mo_7O_{24}/Zr(OH)_4$ (corresponding to 0.5 g MoO_3/g ZrO_2).

It is noteworthy that the surface area of the sample decreases rapidly as long as bulk $Zr_2(MoO_4)_2$ forms.

3.2. WO_3/ZrO_2 system

WO_3/ZrO_2 samples were prepared by impregnating $Zr(OH)_4$ (heated at 10°C) or ZrO_2 (calcined at 500 and 800°C respectively) with a solution of ammonium metatungstate, then calcining at 500 and 800°C respectively. Their specific surface areas are shown in table 2. The results show:

(1) The surface areas of support ZrO_2 obtained by heating pure $Zr(OH)_4$ at 500 and 800°C are 66 and 10 m^2/g respectively. After supporting WO_3, their SA decrease gradually with an increase in WO_3 content, which is in agreement with the general rule of the change in SA of most supported catalysts (table 2, columns B and E).

(2) WO_3/ZrO_2 samples obtained by impregnating $Zr(OH)_4$ are similar to MoO_3/ZrO_2 in the change of their SA with the content of the active component. The

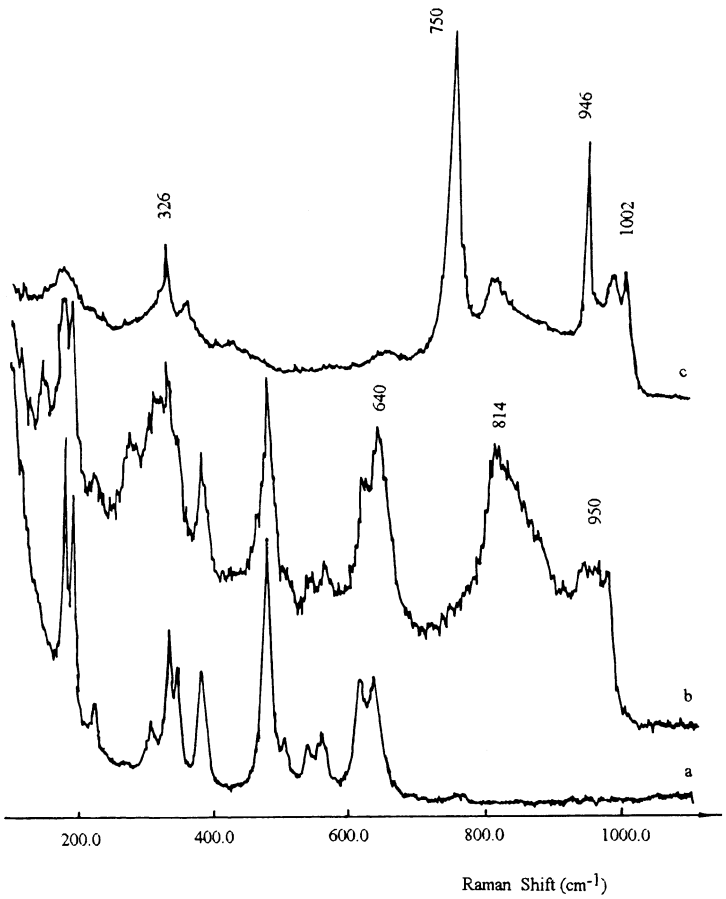

Figure 4. Raman spectra of MoO_3/ZrO_2. (a) ZrO_2 calcined at 550°C; (b) MoO_3/ZrO_2 with 0.09 g MoO_3/g ZrO_2, calcined at 550°C; (c) MoO_3/ZrO_2 with 0.42 g MoO_3/ZrO_2, calcined at 550°C.

Table 2
The surface areas of WO_3/ZrO_2 [a]

WO_3 content ($g/g\ ZrO_2$)	SA (m^2/g)				
	calcined at 500°C		calcined at 800°C		
	A	B	C	D	E
0	66	66	10	10	10
0.05	76	66	44	52	< 10
0.15	175	64	73	50	< 10
0.20	185	63	60	48	< 10
0.30	225	60	57	46	< 10
0.40	227	57	50	42	< 10

[a] A, C: $Zr(OH)_4$ was used as support; B, D: the support was calcined at 500°C.

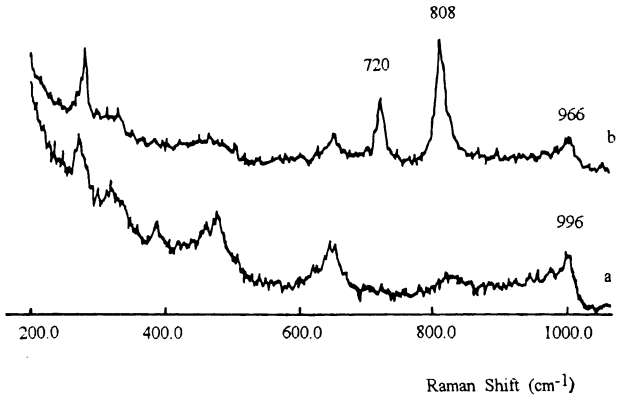

Figure 5. Raman spectra of WO_3/ZrO_2. (a) WO_3/ZrO_2 with 0.15 g WO_3/ZrO_2, calcined at 800°C; (b) WO_3/ZrO_2 with 0.20 g WO_3/ZrO_2, calcined at 800°C.

S_{max} of the samples calcined at 500°C is 3–4 times the SA of pure ZrO_2, and the S_{max} of the samples calcined at 800°C is 7 times the SA of pure ZrO_2 (table 2, columns A and C).

(3) If the support is calcined at a lower temperature (such as 500°C), and then impregnated and calcined again at a higher temperature (such as 800°C), the surface areas of the resultant samples are much larger than those of the samples whose support has been calcined at 800°C (see table 2, columns D and E).

The above results show that the active component WO_3 can stabilize the texture for both $Zr(OH)_4$ and crystallized ZrO_2.

XRD results show that after being calcined at 800°C all of pure $Zr(OH)_4$ turns into monoclinic ZrO_2, whereas if impregnating $Zr(OH)_4$ with enough WO_3 before calcining at 800°C, the ZrO_2 in resultant WO_3/ZrO_2 is still present in tetragonal phase. The situation is quite similar to that of the MoO_3/ZrO_2 system.

In WO_3/ZrO_2 samples, WO_3 is present in a dispersion phase, which is manifested by a rise of a typical broad band at $\sim 996\ cm^{-1}$ in their Raman spectra [16]. If WO_3 content exceeds a certain value, two narrow bands appear at 720 and 808 cm^{-1} attributed to crystalline WO_3 [16]; however, the broad band at $\sim 996\ cm^{-1}$ of the dispersion phase still exists, and its absolute intensity does not change yet (see figure 5). It has been found that the surface area of the sample is maximum when its WO_3 content corresponds to its utmost dispersion capacity on ZrO_2. For WO_3/ZrO_2, the utmost dispersion capacity is close to the geometric monolayer capacity, namely 0.19 g $WO_3/100\ m^2$ support. The authors reported about this in detail in ref. [17].

3.3. CuO/ZrO_2 system

The surface area of CuO/ZrO_2 obtained by impregnating $Zr(OH)_4$ with a solution of $Cu(NO_3)_2$ and then calcining at 500°C is also larger than that of pure ZrO_2 obtained by calcining pure $Zr(OH)_4$ at the same temperature, as shown in table 3. It is obvious that the supported CuO can also stabilize the texture of ZrO_2. The XRD results show that CuO can also delay the crystallization of amorphous ZrO_2 and opposes the t → m transition of ZrO_2. The latter fact was reported by Shimikawabe et al. [18]. In figure 6, one can see that ZrO_2 in the samples with more CuO exists in amorphous state, while in those with less CuO, ZrO_2 is in tetragonal phase, although both of them are calcined at 500°C.

For identifying the state of CuO in CuO/ZrO_2, the XPS peak intensity ratios I_{Cu2p}/I_{Zr3d} as a function of CuO content are determined, as shown in figure 7.

For CuO contents below 0.12 g/g ZrO_2, the slope of the I_{Cu2p}/I_{Zr3d} versus CuO content curve is larger, which indicates all or a great majority of CuO exists on the surface of CuO/ZrO_2. When CuO content is beyond the above value, the slope decreases, which means the additional CuO occurs as a crystalline state or penetrates into the substrate. Since the amount of crystalline CuO detected by XRD is quite low, the later possibility cannot be excluded.

Comparing figure 7 with table 3, we find that the surface area of CuO/ZrO_2 increases gradually and approaches a maximum as the concentration of CuO on the surface increases, and the CuO content of the sample with S_{max} is close to that at the turning point in the XPS I_{Cu2p}/I_{Zr3d} curve. Obviously, it is the CuO dispersed on the surface of ZrO_2 that relaxes the loss of the surface area during calcination.

Table 3
The surface areas of CuO/ZrO_2

CuO content ($g/g\ ZrO_2$)	Surface area ($m^2/g\ ZrO_2$)
0	58
0.04	76
0.06	139
0.09	147
0.11	137
0.14	115

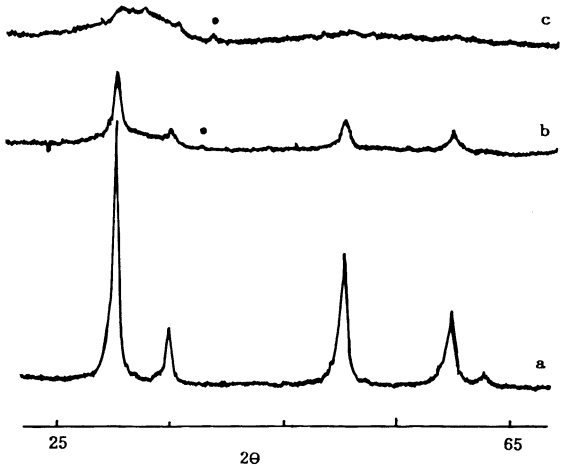

Figure 6. XRD patterns of CuO/ZrO_2. CuO content: (a) 0.04 g CuO/g ZrO_2; (b) 0.11 g CuO/g ZrO_2; (c) 0.22 g CuO/g ZrO_2; (●) Crystalline CuO.

It is also noteworthy that the loading of CuO at the turning point of I_{Cu2p}/I_{Zr3d} versus CuO content is only about half of its geometrical monolayer capacity on ZrO_2, which indicates that CuO can only form a sub-monolayer covering on ZrO_2. This is similar to the case of CuO on γ-Al_2O_3 [19].

The DTA measurements for these samples show that the crystallization temperatures of ZrO_2 in the samples shift up to 527°C (for CuO content of 0.06 g CuO/g ZrO_2) and 607°C (for CuO content of 0.25 g CuO/g ZrO_2), which indicates the dispersed CuO has a strong inhibition effect on the crystallization of ZrO_2.

3.4. SO_4^{2-}/ZrO_2 system

Surface areas of the samples obtained by impregnating $Zr(OH)_4$ with $(NH_4)_2SO_4$ solution and then calcining are also larger than that of pure ZrO_2 calcined at a same temperature, as shown in table 4. Obviously, the surface area of ZrO_2 can also be raised by supporting SO_4^{2-} on it. XRD results show that the supported SO_4^{2-} can also restrain the crystallization of amorphous ZrO_2 and its t → m transition.

Table 4
The surface areas of SO_4^{2-}/ZrO_2

SO_4^{2-} content (g/g ZrO_2)	SA (m^2/g ZrO_2)	
	calcined at 500°C	calcined at 800°C
0	56	27
0.06	125	60
0.08	146	83
0.11	150	91
0.14	156	103
0.17	125	96
0.20	112	80

I_{S2s}/I_{Zr3d} as a function of the content of SO_4^{2-} is shown in figure 8, from which we can see:

(1) The SO_4^{2-} in the sample with a low loading appears on the surface. As SO_4^{2-} content exceeds a certain value, the surface concentration of SO_4^{2-} does not change anymore, which means that the surplus SO_4^{2-} may have escaped as SO_3 during calcination.

(2) For the samples calcined at 500°C, the turning point of the I_{S2s}/I_{Zr3d} versus SO_4^{2-} content curve corresponds to a SO_4^{2-} content of 0.11 g SO_4^{2-}/g ZrO_2, and the corresponding SA is 150 m^2/g ZrO_2. If the samples are treated at 650°C, the turning point corresponds to a SO_4^{2-} content of 0.07 g SO_4^{2-}/g ZrO_2, and its SA is about 80 m^2/g ZrO_2. Both are in good agreement with the utmost monolayer capacity estimated by assuming that SO_3 forms a close-packed layer [2–4], i.e., 0.08 g SO_4^{2-}/100 m^2 ZrO_2. However, we have also noticed that the SO_4^{2-} content in the sample with S_{max} is a little higher than its utmost monolayer capacity. The reason for the occurrence remains to be studied.

3.5. The other systems

The surface areas of all the samples prepared by impregnating $Zr(OH)_4$ with solutions of $Ni(NO_3)_2$, $Fe(NO_3)_2$ and $FeSO_4$ and then calcining at 500°C are

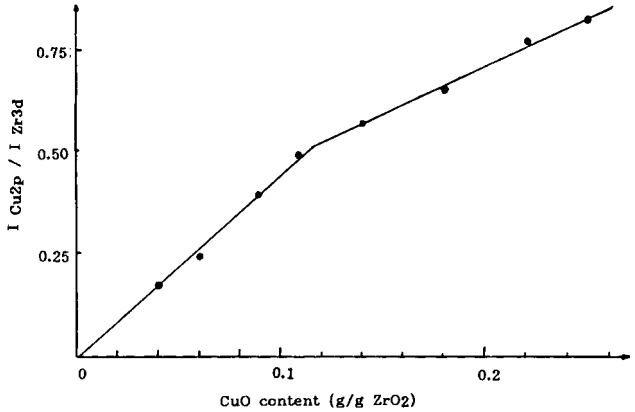

Figure 7. XPS I_{Cu2p}/I_{Zr3d} versus CuO content of CuO/ZrO_2.

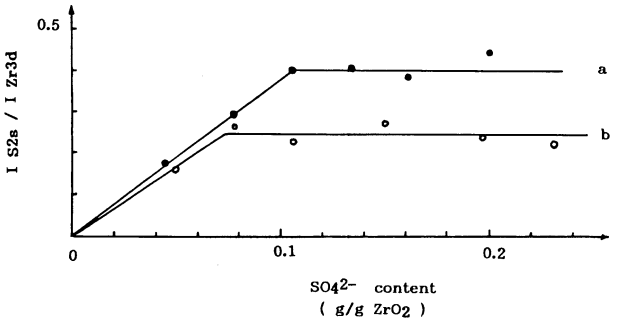

Figure 8. XPS I_{S2s}/I_{Zr3d} versus SO_4^{2-} content of SO_4^{2-}/ZrO_2. Calcination temperature: (a) 500°C; (b) 650°C.

also larger than pure ZrO_2 calcined at the same temperature. A part of the measurements and their corresponding contents of the active components are listed in table 5.

The XRD results show that in NiO/ZrO_2 there is little crystalline NiO, whereas in the other samples no XRD peak of the active components can be detected, which means that all or most part of these active components may occur as dispersion states. In addition, ZrO_2 in these samples is all present in tetragonal modification. These results suggest the universality of the above-mentioned phenomenon.

4. Discussion

It can be seen from the above-mentioned facts that if a layer of active component is covered on colloidal particles of $Zr(OH)_4$ before calcination, the resultant ZrO_2-supported catalysts often have much larger surface areas. The results of the above-listed seven catalysts, without exception, manifest this effect. Using this method, one can increase the surface areas of many ZrO_2-supported catalysts by several times and make them have a favorable comparison with those of the catalysts prepared from some classical supports (such as γ-Al_2O_3, SiO_2).

For all these catalysts under study, the surface areas increase gradually and reach their maxima, then decrease slowly with an increase in the loadings. The active components in all these systems can be dispersed on the surface of ZrO_2, and for each system, the S_{max} occurs when the content of the active component is at its utmost dispersion capacity. Only in SO_4^{2-}/ZrO_2 there appears a bit of discrepancy.

In table 6 the MoO_3 contents of MoO_3/ZrO_2 with S_{max} are listed and compared with those of their theoretical monolayer capacities estimated from their real SA according to the close-packed monolayer model [2,20]. Obviously, they are in good agreement.

In addition, it can be seen that the effectiveness of these components in increasing the surface area is different. MoO_3, WO_3, SO_3 and $FeSO_4$ can form a quite complete monolayer on ZrO_2, while the dispersion capacities of CuO and NiO on ZrO_2 are only about a half of their theoretical values, which means CuO and NiO can only form a sub-monolayer on ZrO_2 [19,21]. The above results show that MoO_3, WO_3, SO_3 and $FeSO_4$ are more effective in increasing the surface area. The reason is that the more completely the surfaces of colloidal grains of ZrO_2 are covered, the more effectively these grains are separated from each other, and the more the surface diffusion of ZrO_2 is suppressed. In this case, the structure of ZrO_2 grain becomes more stable, thus the surface area of ZrO_2-supported catalyst can be maintained better during heat treatment.

However, when the content of an active component exceeds its utmost dispersion capacity, the surplus will appear as crystalline phase to block up the pores of the support (such as in WO_3/ZrO_2) or form a new compound with ZrO_2 at a relatively high temperature (such as $Zr(MoO_4)_2$ in MoO_3/ZrO_2). In these cases, the surface area of a sample will decrease.

The effects of the active components put onto the surface of ZrO_2 in advance can be summed up as follows:

(1) To raise the crystalline temperature of amorphous ZrO_2 obtained from dehydration of $Zr(OH)_4$.

(2) To make ZrO_2 as support preserve in the metastable tetragonal phase at higher calcination temperature instead of turning into the monoclinic phase, and the size of crystalline ZrO_2 grains smaller.

(3) An active component covering on the ZrO_2 calcined and crystallized at a relatively low temperature can still suppress ZrO_2 grains growing up further at higher temperature, and as a result, the trend of a drastic decrease in the surface area of the catalyst during calcination would be relaxed.

Turning amorphous ZrO_2 into crystalline ZrO_2, turning metastable tetragonal into stable monoclinic modification and inter-crystalline sintering among fine grains of ZrO_2 all depend on the stability of the structure of ZrO_2 grains [1,9]. It is by stabilizing the structure of the grains that the active components give rise to the above-mentioned effects and lead to the surface area stabilization observed.

In studies on superplastic structural ceramics it was found that Y^{3+} can stabilize tetragonal ZrO_2 [9]. In addition, it was also pointed out that additive divalent or trivalent cations are enriched at the grain-boundary, which segregate strongly the grain-boundary and lower the grain-boundary mobility and the grain-boundary energy. Obviously, the same principle is coming into play for both the ceramics and the catalyst systems men-

Table 5
The surface areas of some samples

Sample	Content of active component ($g/g\,ZrO_2$)	SA ($m^2/g\,ZrO_2$)
ZrO_2	0	48
NiO/ZrO_2	0.14	80
Fe_2O_3/ZrO_2	0.10	87
$FeSO_4/ZrO_2$	0.19	143

Table 6
The maximum specific surfaces of MoO_3/ZrO_2 and their corresponding MoO_3 contents

Calcination temp. (°C)	S_{max} ($m^2/g\,ZrO_2$)	MoO_3 content ($g/g\,ZrO_2$)	Close-packed monolayer capacity ($MoO_3/g\,ZrO_2$)
450	310	0.31	0.37
550	225	0.27	0.27
600	195	0.24	0.23
750	100	0.12	0.12

tioned above. Recently, Y^{3+} and La_2O_3 were also used for stabilizing tetragonal ZrO_2 in some catalyst systems [22].

It should be pointed out that since the chemical properties of $Zr(OH)_4$ are more active than those of ZrO_2, the probability of the surface or bulk reaction between $Zr(OH)_4$ and active component cannot be ignored. Therefore, the state of the active component in the catalyst prepared from $Zr(OH)_4$ might change to some extent. For example, it has been described above that in Raman spectra of MoO_3/ZrO_2 prepared from $Zr(OH)_4$ a new characteristic broad band at about 812 cm^{-1} occurs, which is attributed to a Mo–O–Zr surface species, and as MoO_3 content exceeds its utmost dispersion capacity the crystalline $Zr(MoO_4)_2$ appears after calcination at 550°C. Whereas, for MoO_3/ZrO_2 prepared from crystallized ZrO_2 the Raman band at $\sim 812\ cm^{-1}$ does not appear, and the surplus MoO_3 still exists as crystalline MoO_3 even if calcined at higher temperature [15]. Therefore, it can be expected that there might be some differences between a catalyst from ZrO_2 and that from $Zr(OH)_4$ in their catalytic behavior. As the interaction between the support and an active component is strong, the difference would become more obvious. It is a typical example that MoO_3/ZrO_2, WO_3/ZrO_2 and SO_4^{2-}/ZrO_2 prepared from $Zr(OH)_4$ possess superacidity but those prepared from ZrO_2 do not [6,7]. So using the method recommended in this paper to prepare a catalyst, one must pay attention to whether its properties in adsorption and catalysis change or not.

In some cases, we suggest a compromise proposal, namely, calcining $Zr(OH)_4$ at a relatively low temperature to turn it into ZrO_2 with a quite high surface area, then impregnating it with the solution of an active component or its precursor and calcining it again at the high temperature required in a desired application. Since during the second calcination the active component can still suppress grain growth of ZrO_2 and the inter-grain sintering, one can obtain a catalyst whose specific surface is larger and whose change in surface properties is slight.

We find that the above-mentioned effects also exist in TiO_2 or Al_2O_3-supported catalysts to some extent, which will be reported subsequently.

Acknowledgement

The authors acknowledge China's National Science Foundation and National Science and Technique Committee for their generous support for this work. We are grateful to Yu Zhou who determined the XPS peak intensity ratio. Thankful acknowledgements are due to You-chang Xie, Lin-lin Gui, Xiao-hai Cai, Gang Yu and Zhi-guo Ren for their help.

References

[1] P.D.L. Mercera, J.G. van Ommen, E.B.M. Doesburg, A.J. Burggraaf and J.R.H. Ross, Appl. Catal. 57 (1990) 127.
[2] Y.C. Xie and Y.Q. Tang, Adv. Catal. 37 (1990) 1.
[3] Y.C. Xie, L.L. Gui, Y.J. Liu, B.Y. Zhao, N.F. Yang, Y.F. Zhang, Q.L. Guo, L.Y. Duan, H.Z. Huang, X.H. Cai and Y.Q. Tang, in: *Proc. 8th Int. Congr.on Catalysis* (Verlag Chemie, Weinheim, 1984) 5, 147.
[4] Y.C. Xie, L.L. Gui, Y.F. Zhang, B.Y. Zhao, N.F. Yang, Q.L. Guo, L.Y. Duan, H.Z. Huang, X.H. Cai and Y.Q. Tang, in: *Adsorption and Catalysis on Oxide Surface*, eds. M. Che and G.C. Bond (Elsevier, Amsterdam, 1985) p. 139.
[5] B.Y. Zhao, H.Z. Liu, L.L. Gui and Y.Q. Tang, J. Catal. (China) 8 (1987) 413.
[6] K. Arata and M. Hino, Mater. Chem. Phys. 26 (1990) 213.
[7] K. Arata, Adv. Catal. 37 (1990) 165.
[8] A. Cimino, D. Cordischi, S. De Rossi, G. Ferraris, D. Gozzoli, G. Minelli, M. Occhiuzzi and M. Valigi, J. Catal. 127 (1991) 744.
[9] I. Wei and X. Liang An, J. Am. Ceram. Soc. 73 (1990) 2585.
[10] C. Xu, J. Tamaki, N. Miura and N. Yamazoe, J. Mater. Sci. Lett. 8 (1989) 1092.
[11] C. Xu, J. Tamaki, N. Miura and N. Yamazoe, Sensors and Actuators B 3 (1991) 147.
[12] Keshavaraja, B.S. Jayashri and A.V. Ramaswamy, Sensors and Actuators B 3 (1995) 75.
[13] J. Medema, C. van Stam, V.H.J. de Beer, A.J.A. Konings and D.C. Koningsberger, J. Catal. 53 (1978) 386.
[14] H. Knözinger and H. Jeziorowski, J. Phys. Chem. 82 (1978) 2002.
[15] B.Y. Zhao, X.Y. Wang, H.R. Ma and Y.Q. Tang, Mol. Catal. A 108 (1996) 167.
[16] S.S. Chan, I.E. Wachs, L.L. Murrell and N.C. Dispenziere, J. Catal. 92 (1985) 1.
[17] B.Y. Zhao, X.P.Xu, J.M. Gao and Y.Q. Tang, J. Raman Spectrosc. 27 (1996) 549.
[18] M. Shimokawabe, H. Asakawa and N. Takezawa, Appl. Catal. 59 (1990) 45.
[19] B.Y. Zhao, Y.F. Zhang, L.Y. Duan, Y.C. Xie and Y.Q. Tang, J. Catal. (China) 39 (1982) 101.
[20] Liu, Y.C. Xie, J. Ming, J. Liu and Y.Q. Tang, J. Catal. (China) 39 (1982) 262.
[21] Zhang, Y.C. Xie, Y. Zhang, D.L. Zhang and Y.Q. Tang, Sci. Sin. Ser. B (Chin. Ed.) 8 (1986) 805.
[22] P.D.L. Mercera, J.G. van Ommeren, E.B.M. Doesburg, A.J. Burggraaf and J.R.H. Ross, Appl. Catal. 78(1991) 79.